Collective motion in Ar+Pb collisions at beam energies between 400 and 1800 MeV/nucleon

D. Beavis,[1],* R. Bock,[2] R. Brockmann,[2] P. Danielewicz,[3] S.Y. Fung,[1] J.W. Harris,[4] D. Keane,[5] Y.M. Liu,[1],† G. Odyniec,[4] H.G. Pugh,[4],‡ R.E. Renfordt,[6] A. Sandoval,[2] D. Schall,[2] L.S. Schroeder,[4] R. Stock,[6] H. Ströbele,[6] M.A. Vient,[1],§

[1] *Department of Physics, University of California, Riverside, California 92521*
[2] *Gesellschaft für Schwerionenforschung, D6100 Darmstadt, Germany*
[3] *National Superconducting Cyclotron Laboratory and Physics & Astronomy Department, Michigan State University, East Lansing, Michigan 48824*
[4] *Lawrence Berkeley Laboratory, University of California, Berkeley, California 94720*
[5] *Department of Physics, Kent State University, Kent, Ohio 44242*
[6] *Fachbereich Physik, Universität Frankfurt/Main, Germany*

(Received 3 June 1991)

The energy dependence of rapidity distributions and flow effects was studied in central Ar+Pb collisions at 400, 800, and 1800 MeV/nucleon using a streamer chamber. Rapidity distributions for protons and pions are found to have a Gaussian shape whereas those for deuterons exhibit a two-peak structure at the two higher energies. The average in-plane transverse momentum per nucleon and per event shows saturation of flow around 800 MeV/nucleon for this asymmetric system. The aspect ratio of the sphericity tensor is closely correlated with the flow angle. This correlation appears to be independent of beam energy. The number of participating nucleons in central collisions varies from 213 at 400 to 135 at 1800 MeV/nucleon indicating that at the lowest energy almost the entire target nucleus participates in the collision.

PACS number(s): 25.75.+r

I. INTRODUCTION

The bulk properties of nuclear matter are the subject of intense studies both experimentally and theoretically. In astrophysics, the collapse of stars into neutron matter or their explosion into supernovae can be understood only if the behavior of nuclear matter under such extreme conditions is known. This implies the understanding of soft hadronic interactions and their connection to the equation of state (EOS) of nuclear matter. The freeing of quark and gluon degrees of freedom at high temperature or density would reveal itself as a phase transition in the EOS. The resulting efforts to determine the equation of state of nuclear matter and the more general aspect of producing high-energy densities over extended regions have led to a series of experiments to study collisions between relativistic heavy ions at the Synchrophasotron in Dubna and at the Bevalac in Berkeley. One of the main results of these investigations was the discovery of the hydrodynamical response of nuclear matter to collision shocks evident in the transverse flow of nuclear fragments [1]. The behavior of nuclear matter in such a hot and compressed phase was studied by Chapline *et al.* and Scheid *et al.* [2] as early as 1973/74. Since then, a large number of experimental results from various groups and research facilities has confirmed and supplemented the early findings. However, no quantitative theoretical picture of the bulk properties of nuclear matter at high densities has evolved. The complexity of the macroscopic and microscopic models, which include among others the effects of the nuclear equation of state [3], has increased rather than given way to a universal picture of the process of compressing and heating nuclear matter. In order to constrain the various parameters and verify the different assumptions and approximations in the models, systematic experimental studies are needed which provide quantitative information on the transverse flow and the nuclear stopping power as a function of beam energy and projectile/target mass.

In this paper, measurements of central Ar+Pb collisions at 400, 800, and 1800 MeV/nucleon will be presented. These measurements combine data-acquisition efforts of both the Riverside and GSI/LBL Streamer Chamber groups. Results on nucleons and nuclear fragments at 1800 MeV/nucleon will be given for the first time, whereas the measurements at 400 [4] and 800 MeV/nucleon [5] were the subject of earlier work. The energy dependence of rapidity distributions and transverse flow will be presented in this paper. The rapidity

*Present address: Brookhaven National Laboratory, Upton, NY 11973.
†Present address: Department of Physics, Harlin Institute of Technology, Harlin 150006, PRC.
‡Deceased.
§Present address: Physics Department, University of California, Irvine, CA 92717.

distributions of pions, protons and deuterons provide information about thermalization and the stopping power of nuclear matter. The transverse momentum analysis method [6] is used to determine the double-differential rapidity and transverse momentum dependence of the mean in-plane transverse momentum of all protons.

Our analysis shows that the pions have a nearly Gaussian rapidity distribution which is broader than the rapidity gap between target and projectile, and that is centered at the participant center-of-mass rapidity. The large widths are in particular expected for pions from $\Delta(1236)$ decays [7]. As for the nucleons, different behaviors are observed for the free protons than for those bound in clusters. The rapidity distributions of the former reflect the asymmetry of projectile and target masses with little impact parameter dependence. Their widths are compatible with the assumption of a thermal source of protons. Overall the distributions are slightly asymmetric and exhibit no structure. Deuterons, however, develop a two-peak structure at intermediate impact parameters above 4 fm. This, with the absence of a similar structure in the proton distributions, may be understood in conjunction with collective flow: coalescence is suppressed in those regions of phase space where the motion is mainly chaotic (close to the c.m. rapidity) whereas nuclear fragment formation is favored in the low-entropy domain of ordered motion.

If the transverse momentum analysis is used to determine the center of mass, the effective number of nucleons participating in the collision is highest at 400 MeV/nucleon and approaches the minimum value as given by clean cut geometry for central collisions at 1800 MeV/nucleon. The total transverse momentum transfer from the projectile to the target hemisphere reaches a maximum at intermediate beam energies indicating a saturation of flow effects. This is also seen in the mean in-plane transverse momentum of protons.

The experimental procedure is described in the following section. Section III contains the results and the discussion.

II. EXPERIMENTAL PROCEDURE

Details of the experimental procedures and data-acquisition techniques have been presented in previous publications. In this section we characterize the three data samples and describe the three different and complementary methods of particle identification. Semicentral collisions of ^{40}Ar projectiles with Pb_3O_4 targets were recorded with the Bevalac Streamer Chamber facility. The target thicknesses were 1.17, 1.13, and 1.17 g/cm^2 for 400, 800, and 1800 MeV/nucleon, respectively. A forward particle veto trigger together with an off-line multiplicity cut in the number of participant protons was used to reject ^{40}Ar+^{16}O events as well as all peripheral collisions. This selection corresponds approximately to a trigger cross section of 1 b and has resulted in 158, 958, and 925 analyzed events at 400, 800, and 1800 MeV/nucleon, respectively.

The momenta of charged particles were measured in the streamer chamber operating in a magnetic field of 1.3 T . Mass identification by energy loss measurements was possible only in limited regions of phase space: $50 < p_{\rm lab} < 350$ MeV/c for pion-proton separation and $800 < p_{\rm lab} < 1700$ MeV/c for proton-deuteron separation (I). Since knowledge of the complete four vector of all (charged) particles is necessary, two additional procedures were developed to assign masses to individual particles. Composite particles could be identified, if their magnetic rigidity lied outside the proton phase space (II): i.e. tritons with laboratory momenta $p_{\rm lab} > 2p_{\rm beam}$/nucleon and deuterons (including a 10% admixture of ^{3}He and tritons) with $p_{\rm beam}$/nucleon $< p_{\rm lab} < 2p_{\rm beam}$/nucleon. Remaining ambiguities were resolved using a Monte Carlo procedure (III) by assigning masses to individual particles on the basis of the observation [4] that coalescence coefficients are independent of momentum and angle. The coalescence coefficients for deuterons and tritons were derived from the data in the region where procedure I or II are applicable. The last method provides correct identification on the average but cannot be applied on a particle-by-particle basis. In order to illuminate the corresponding bias we note that, if composite particles are mistaken as nucleons, a high transverse momentum and consequently a high contribution to the flow will be observed. On the other hand, a nucleon which is treated like a composite particle will be assigned a too low transverse momentum. Since these over- (under-) estimates are not correlated with the event plane, they will smear out and reduce the flow effects. As a result of the particle identification and mass assignment procedures the deuteron sample at the two higher beam energies is nearly bias-free for $p_{\rm lab} > 1000$ MeV/c, whereas the protons are contaminated by up to 20% deuterons from lower rapidities. Both yields have a systematic uncertainty of 7%. Below $p_{\rm lab} = 1000$ MeV/c masses were assigned to fragments on a statistical basis only with a deuteron-to-proton ratio of d/p=0.5. The contamination of baryons by positively charged pions is negligible. No attempt was made to identify particles with $Z > 1$. There is some contamination of the deuteron sample from tritons and ^{3}He. However, distortions in rapidity and in-plane transverse momentum caused by ^{3}H and ^{3}He are approximately the same but opposite in sign. The resulting systematic error in the mean in-plane transverse momenta is estimated to be approximately 5%. ^{4}He particles ($\approx$5% contamination) are also contained in the deuteron sample but are treated correctly in the variable momentum per nucleon, since they have the same Z/A ratio as deuterons. Only the number of participating protons is slightly underestimated by treating ^{4}He as deuterons. Heavier fragments can be completely neglected above rapidities of approximately 0.4, since their abundance is below the 1% level outside the target fragmentation region in central collisions. At the lowest beam energy only procedures II and III were used [4] and the small contamination from positively charged pions (0.03 pion per proton) was neglected.

III. RESULTS

The effective trigger cross section for the event samples at all beam energies was $\approx$ 1 b. This corresponds

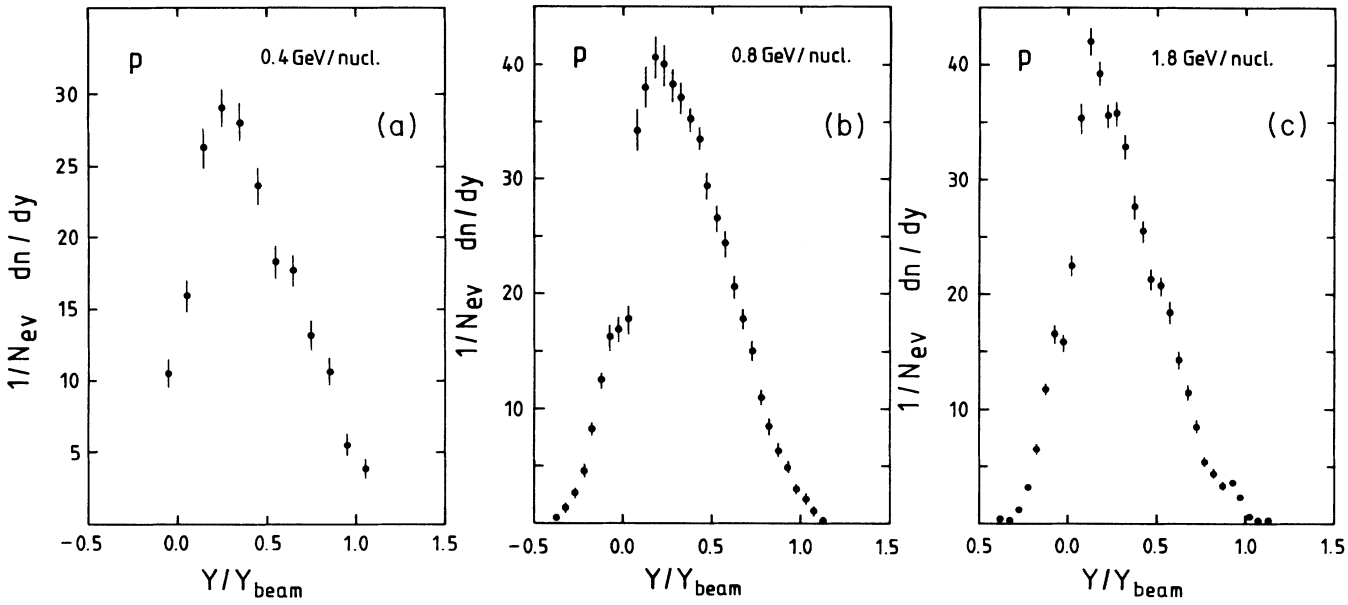

FIG. 1. Rapidity distribution of protons in central Ar+Pb collisions at 400 MeV/nucleon (a), 800 MeV/nucleon (b), and 1800 MeV/nucleon (c). The vertical scale gives the number of particles per unit rapidity per event; the abscissa is the rapidity normalized to beam rapidity.

to the most central 28% of all inelastic collisions. In a geometrical model this cross section can be related to the impact parameter range $0.0 < b < 5.5$ fm with an average b of 3.7 fm. Complete overlap of the projectile with the target occurs for $b < 3$ fm. The assumption of straight lines for the trajectories of the colliding nucleons leads to an average of less than four projectile spectator nucleons per event. Thus, the present data sample consists on the average of central Ar+Pb collisions with less than two projectile spectator protons. This small number will be neglected in the determination of the number of participating nucleons from the experimental data. The mean

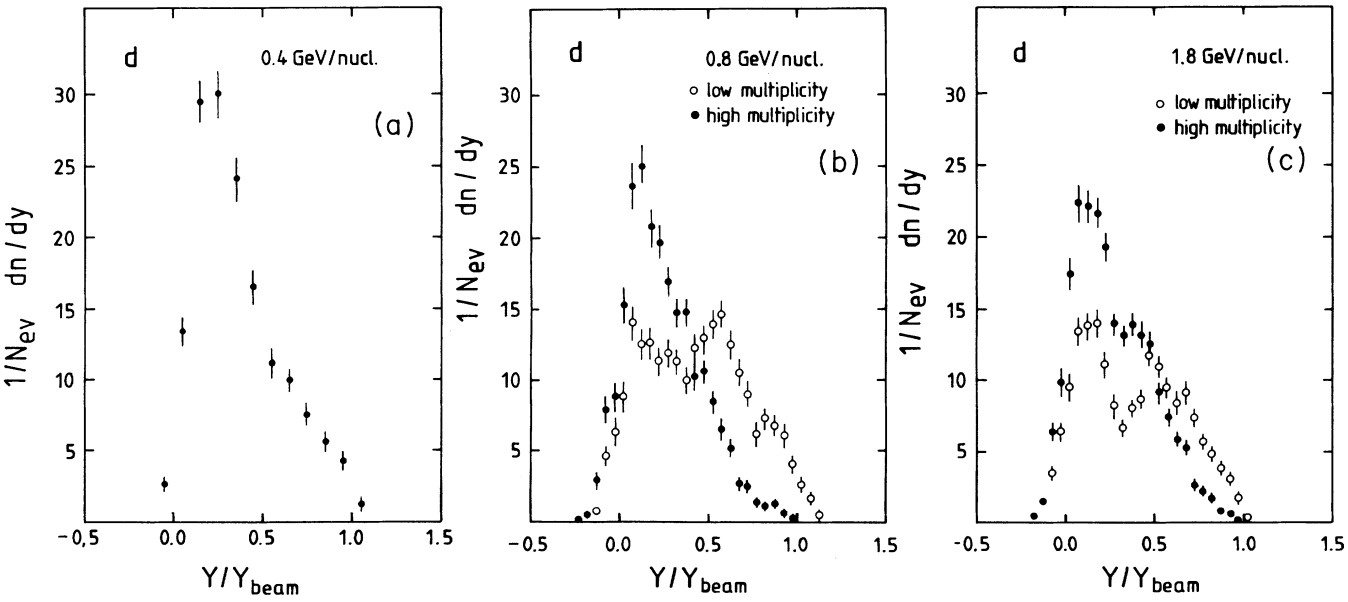

FIG. 2. Rapidity distribution of deuterons in central Ar+Pb collisions at 400 MeV/nucleon (a), 800 MeV/nucleon (b), and 1800 MeV/nucleon (c). At the two higher energies low (LOM) and high (HIM) multiplicity events are analyzed separately. The vertical scale gives the number of particles per unit rapidity per event; the abscissa is the rapidity normalized to beam rapidity.

number of participating protons, either free or bound in composite nuclei, was determined by excluding proton spectators with laboratory momenta of less than 280 MeV/c. It was found to be 40, 46, and 53 at the three energies 0.4, 0.8, and 1.8 GeV/nucleon, respectively. These will be called participant protons and represent a lower limit for the true number of protons participating in the collision.

The rapidity distributions of protons, deuterons, and pions and the result of a systematic flow analysis will be presented below. The choice of rapidity to represent the longitudinal degree of freedom ensures scale invariance under Lorentz transformation. However, a comparison of rapidity distributions measured at different incident energies may be misleading, since it is unclear whether the moments of the distributions should be independent of energy or scale with the available rapidity interval. The first would be the case, if the distributions resulted from a thermalized system at constant temperature. The second would be the result of a simple scaling behavior. For the sake of simplicity we have chosen to normalize rapidity to beam rapidity (y_{beam}). It should be noted, however, that so far this choice is not justified by any physics argument.

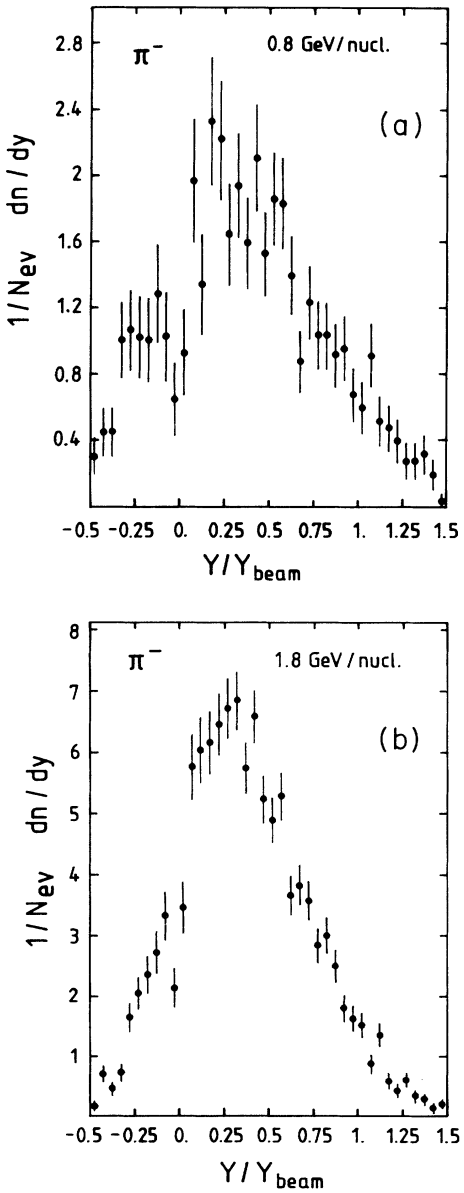

FIG. 3. Rapidity distribution of negatively charged pions in central Ar+Pb collisions at 800 MeV/nucleon (a) and 1800 MeV/nucleon (b).

A. Rapidity distributions

The proton rapidity densities per unit of rapidity are presented in Fig. 1 as a function of normalized rapidity $y' = y/y_{\text{beam}}$ for the three incident energies. The distributions are similar and asymmetric with respect to $y'=0.5$ due to the asymmetry of the projectile/target configuration. Translating the width of the proton rapidity distribution into a temperature leads to 50, 85, and 150 MeV at the three energies. The deuteron rapidity densities are presented in Fig. 2 for the three incident energies. Their shapes exhibit a more complicated structure than those of the protons. A clear structure forward from $y'=0.25$ develops at the higher energies. This effect is centrality dependent. We have, therefore, applied an additional off-line selection on multiplicity, for the 800 and 1800 MeV/nucleon data, selecting impact parameters below [open symbols in Figs. 2(b) and 2(c)] and above $\approx$ 3.5 fm [solid dots in Figs. 2(b) and 2(c)]. The two-peak structure is clearly less pronounced for central collisions and leads to a d/p ratio which coincides with the well-established ratio of $\approx$ 0.5 at low rapidity and rises to $d/p=1$ near projectile rapidities. We have verified that the dip is not caused by our particle identification method. In fact it comes about because deuterons with low transverse momentum are suppressed around $y'=0.35$. The dip appears at rapidities where the least flow is detected (see below). The structure is most pronounced at 1800 MeV/nucleon and disappears at 400 MeV/nucleon. At the lowest energy, the particle identification method smears out any fine structure in the rapidity spectra. No signal of an appreciable amount of proton or deuteron spectators is visible in these semicentral collisions at any energy.

The pion rapidity distributions are presented in Fig. 3. Only the two higher energies were analyzed due to the small number of produced pions near threshold in the 400 MeV/nucleon data. The distributions are nearly symmetric with respect to the participant nucleons c.m.s. and have Gaussian shape. The widths are broader than those from the nucleons and are in qualitative agreement with the assumption that most of the pions originate from $\Delta(1236)$ decays. Alternatively the pion temperature can be estimated from the widths of the y' distributions by fitting the form $\exp(-m_\perp \cosh y/T)$ to the rapidity distribution dn/dy with $m_\perp = \sqrt{m^2 + p_\perp^2}$ being the transverse mass and T the temperature. We find 45 ± 20 and 66 ± 20 MeV at 800 and 1800 MeV/nucleon, respectively. All rapidity distributions have a narrow dip at $y'=0.0$ due to particle absorption in the target.

B. The transverse momentum analysis

The systematics of flow effects in Ar+Pb collisions have been studied as a function of beam energy using the transverse momentum method. In earlier work, the experimental data at 800 MeV/nucleon were analyzed for deuterons only [5]. Here we have included all protons, whether free or bound in clusters (mainly d, t, He). The results of the analysis are presented in terms of the mean in-plane transverse momentum as a function of rapidity and p_T. Averaging has been done either per nucleon or per event and per rapidity/p_T interval.

The dependences of the mean in-plane transverse momentum per nucleon $\langle p_x \rangle$ and per event dP_x/dy on rapidity are shown in Fig. 4 for the three energies. The behavior of $\langle p_x \rangle(y)$ (upper row) differs from the common S shape because of the asymmetry in the collision geometry. The intercept of the curve at $\langle p_x \rangle = 0.0$ can be identified with the rapidity of the center-of-mass frame. This intercept is shifted to low rapidities with respect to the nucleon-nucleon c.m. at y'=0.5 . Thus the forward hemisphere of the c.m. frame covers a large fraction of the total rapidity interval. Below y'=0.25, the flow observables are less reliable due to lack of mass identification on a particle-by-particle basis, as described above. The rise of $\langle p_x \rangle$ with rapidity becomes more pronounced with increasing beam energy, with $\langle p_x \rangle_{\max}$ exceeding 150 MeV/c at the highest energy.

In the literature to date two measures of transverse flow have been used: $\langle p_x \rangle_{\max}$, and the slope of $\langle p_x \rangle(y)$ near $p_x = 0.0$ [8]. The very asymmetric systems Ar+Pb and Ar+BaI_2 [9] exhibit the highest flow reported so far, using either definition, reaching 150 MeV/c for $\langle p_x \rangle_{\max}$ whereas in the heavy Au+Au system the Plastic Ball finds $\langle p_x \rangle_{\max}$ smaller than 100 MeV/c [10, 1]. The increase of $\langle p_x \rangle_{\max}$ with energy is stronger between 400 and 800 MeV/nucleon than between 800 and 1800 MeV/nucleon. This trend is further accentuated in the mean in-plane transverse momentum per event dP_x/dy (lower row in Fig. 4): both $dP_x/dy_{\max}$ and P_x, the total momentum transfer per event which is the integral in the forward hemisphere of the c.m.s. ($y' > y_{px=0}$, see Table I), are highest at 800 MeV/nucleon.

The intercepts of both $\langle p_x \rangle(y)$ and dP_x/dy with the rapidity axis (see Fig. 4) determine the c.m. rapidity defined by vanishing transverse flow at $y_{\text{c.m.}}$. This constitutes an independent determination of the c.m. velocity, which differs by less than 0.2 unit of rapidity from the result from balancing the longitudinal momenta of all measured nucleons with transverse momenta above 250 MeV/c (see Ref. [5] and Table I). From the corresponding velocities one can compute the average number of participating target nucleons provided that all projectile nucleons interact (i.e., complete geometrical overlap of the projectile with the target). This latter condition is nearly fulfilled as mentioned above. We obtain 211, 156, and 133 participating nucleons from both projectile and target at 400, 800, and 1800 MeV/nucleon, respectively. In the simple clean cut geometrical model central collisions lead to approximately 99 interacting nucleons. Direct determination of this number from the proton mul-

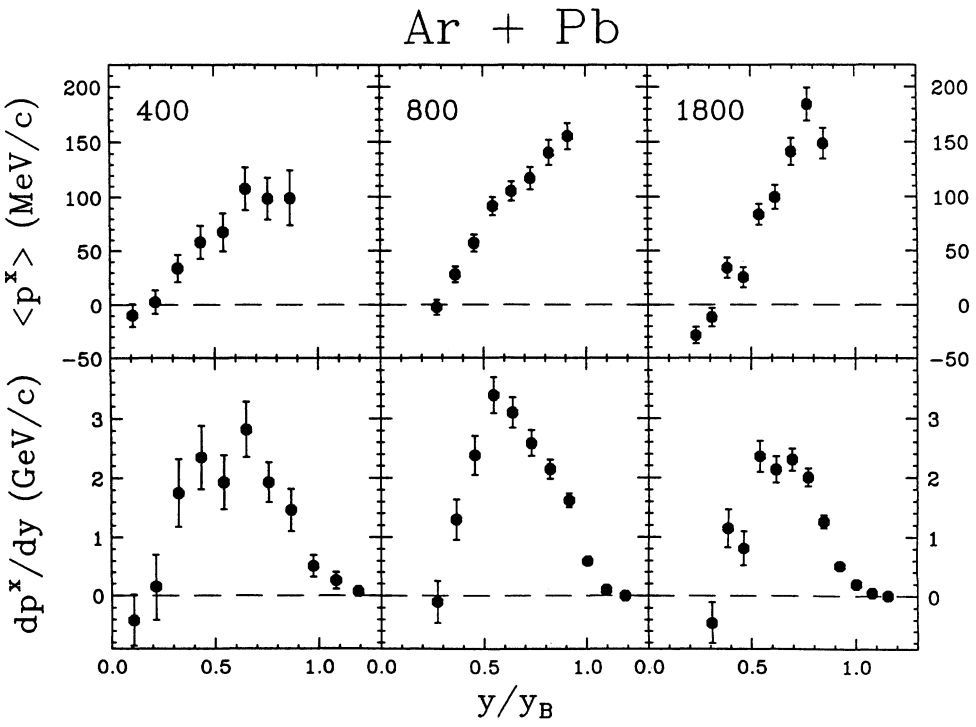

FIG. 4. Average transverse momentum component per event (lower row) and average transverse momentum component per nucleon (upper row) in the reaction plane as function of normalized rapidity in central Ar+Pb collisions at 400, 800, and 1800 MeV/nucleon.

TABLE I. Global observables for central Ar+Pb collisions at three beam energies. Intersect denotes the value of rapidity for which the mean in-plane transverse momentum changes sign and thus vanishes (see text). Total momentum transfer is to protons in the rapidity region above the intersect. The momentum per nucleon is evaluated from protons with rapidities greater than 0.1, 0.15, and 0.3 above the intersect for beam energy of 400, 800, and 1800 MeV/nucleon, respectively. In the definitions of the aspect ratios f_i (i=1,3) denote the magnitude of the three main tensor axis.

Beam energy (MeV/nucleon)	400	800	1800
σ(reaction) (b)	1.0	1.0	1.0
⟨Partic. protons⟩ ($p_{\rm lab}$ > 280 MeV/c)	40	46	53
Partic. nucleons from clean cut geometry	99	99	99
⟨Partic. nucleons⟩ from intersect	211	156	133
y of intersect	0.18	0.34	0.58
$v_{\rm c.m.}$ from $\sum p_{\rm long}$=0	0.34	0.47	0.59
Average in-plane transverse mom. $\overline{\langle p_x \rangle}$ (MeV/c)	74 ± 7	96 ± 4	108 ± 4
Total mom. transfer per event P_x (GeV/c)	1.27 ± 0.16	1.89 ± 0.10	1.68 ± 0.10
Θ(flow) (deg)	16.5 ± 0.8	19.7 ± 0.9	14.8 ± 0.7
Aspect ratio [$r = 2f_3/(f_1 + f_2)$]	2.30 ± 0.03	1.91 ± 0.03	2.27 ± 0.04
Aspect ratio ($r_{31} = f_3/f_1$)	2.46 ± 0.06	2.10 ± 0.06	2.32 ± 0.05
Aspect ratio ($r_{21} = f_2/f_1$)	1.14 ± 0.03	1.20 ± 0.05	1.05 ± 0.04

tiplicity (given above) and the Z/A ratio of the colliding nuclei yield 102, 115, and 135 interacting nucleons at the three energies. These numbers represent a lower limit, since particles with $p_{\rm lab}$ <280 MeV/c are not included, and He fragments are treated as singly-charged particles thus contributing only one proton. Both effects will be stronger at lower energies. At 1800 MeV/nucleon the two approaches show good agreement with each other, while the result of clean cut geometry is low by about 10%. Large differences develop with decreasing energy. At the lowest energy it seems that the target nucleus as a whole interacts with the projectile. This may be attributed to the lower relative velocity of the colliding nuclei, which allow rescattering of the participating nucleons with the surrounding cold spectator matter at the lowest energy. The dip in the rapidity distribution of the deuterons in Fig. 2 occurs at the same c.m. rapidity as the intercept. Here the directed flow vanishes, the chaotic motion prevails and coalescence is suppressed. Away from the c.m. rapidity the directed flow increases steeply and deuteron formation is favored.

The double-differential distribution of the mean in-plane transverse momentum ($d^2P_x/dy\,dp_T$) is displayed as function of $y/y_{\rm beam}$ and $(p_T/m)/y_{\rm beam}$ in Fig. 5. Its maximum reaches the highest value for the 800 MeV/nucleon data already seen in the projection onto the longitudinal axis dP_x/dy. The position of the maximum is approximately independent of incident energy. It should be noted, however, that $y_{\rm beam}$ increases with increasing incident energy. One may conclude from Fig. 5 that most of the momentum transfer is carried by particles around $y = 0.6y_{\rm beam}$. This corresponds to rapidities of 0.6, 0.7, and 1.1 at the three energies, respectively. The corresponding trend in $(p_T/m)/y_{\rm beam}$ is a slight drop of the position of the maximum in differential momentum transfer from 0.4 to 0.35.

C. Discussion

The beam energy dependence of the flow effects is demonstrated in two observables: (i) the total transverse

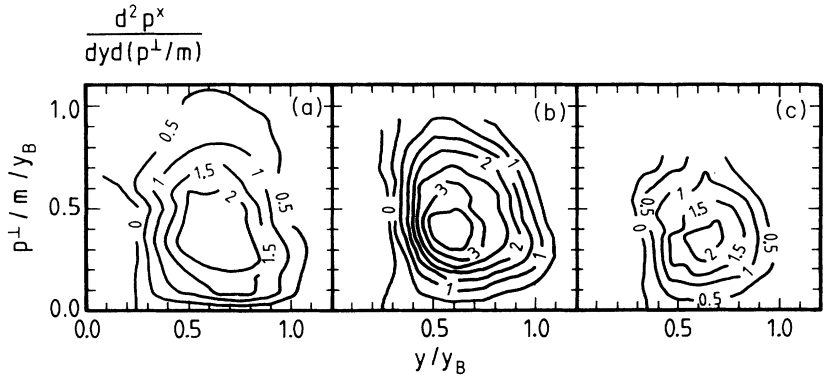

FIG. 5. Double-differential distribution of the net transverse momentum component in the reaction plane as function of normalized rapidity and normalized p_T in central Ar+Pb collisions at 400, 800, and 1800 MeV/nucleon. At the lowest energy 327 events were used for the contour plot to increase the statistics to an acceptable level. No significant difference in this observable was found by the implicit increase of the impact parameter.

momentum transfer (from the backward to the forward hemisphere of the c.m. frame) P_x and (ii) the average transverse momentum per nucleon in the forward hemisphere $\overline{\langle p_x \rangle}$. Both variables consistently rise faster between 400 and 800 MeV/nucleon than between 800 and 1800 MeV/nucleon (cf. Table I). At the highest beam energy P_x shows a moderate decline at the two standard deviations level. This energy dependence of the flow is summarized in Fig. 6. The $\langle p_x \rangle$ averaged over the forward hemisphere of the c.m.s. rises monotonically with E_{beam} showing a clear tendency to level-off at the highest energy. Results on central Ar+BaI_2 [9], Ar+KCl [5, 7, 9], Ca+Ca [10], and Ar+V [11] collisions are given for comparison. For this light symmetric configuration a linear rise with beam energy from $\overline{\langle p_x \rangle}$=30 MeV/$c$ at 400 MeV/nucleon to 95 MeV/c at 1800 MeV/nucleon is observed. The flow in the asymmetric system Ar+Pb, presented here, levels off above 800 MeV/nucleon, with data on an intermediate mass target (BaI_2) [9] exhibiting a somewhat higher $\overline{\langle p_x \rangle}$ at 1200 MeV/nucleon although compatible within two standard deviations with the Ar+Pb systematics.

The Plastic Ball and Diogene groups have used the slope of the S-shaped $\langle p_x \rangle(y)$ dependence to present their flow measurements. The Plastic Ball data [8] are presented in units of normalized rapidity ($y/y_{\text{c.m.}}$). The symmetric systems analyzed so far range from Ne+NaF to Au+Au. A significant increase of the flow with energy is seen by the Plastic Ball below 400 MeV/nucleon. In the beam energy interval studied here, the variation of the flow is small, ranging from 10% in Ca+Ca to 15% in Au+Au. This is in strong contrast to the $\overline{p_x}$ observable used in the streamer chamber analysis which shows a factor of 3 increase even for the low-mass system Ar+KCl (see Fig. 6). An estimation of the slope parameter from streamer chamber data on Ar+KCl at 800 and 1200 MeV/nucleon gives 100 MeV/c in agreement with the Plastic Ball finding for Ca+Ca at the same energy.

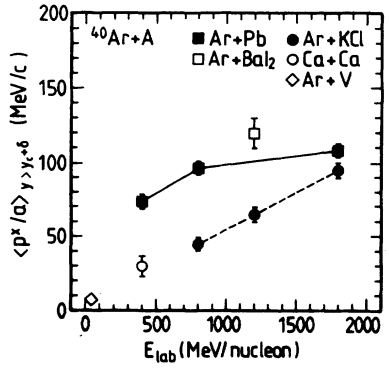

FIG. 6. Average transverse momentum per nucleon in the reaction plane in the forward hemisphere of the c.m. system as a function of beam energy for various projectile/target configurations. The Ar+BaI_2 and Ar+KCl data at 1200 MeV/nucleon are from Ref. [9], the remaining Ar+KCl data are from [5, 6]; Ca+Ca data are from [10] and Ar+V data are from [11].

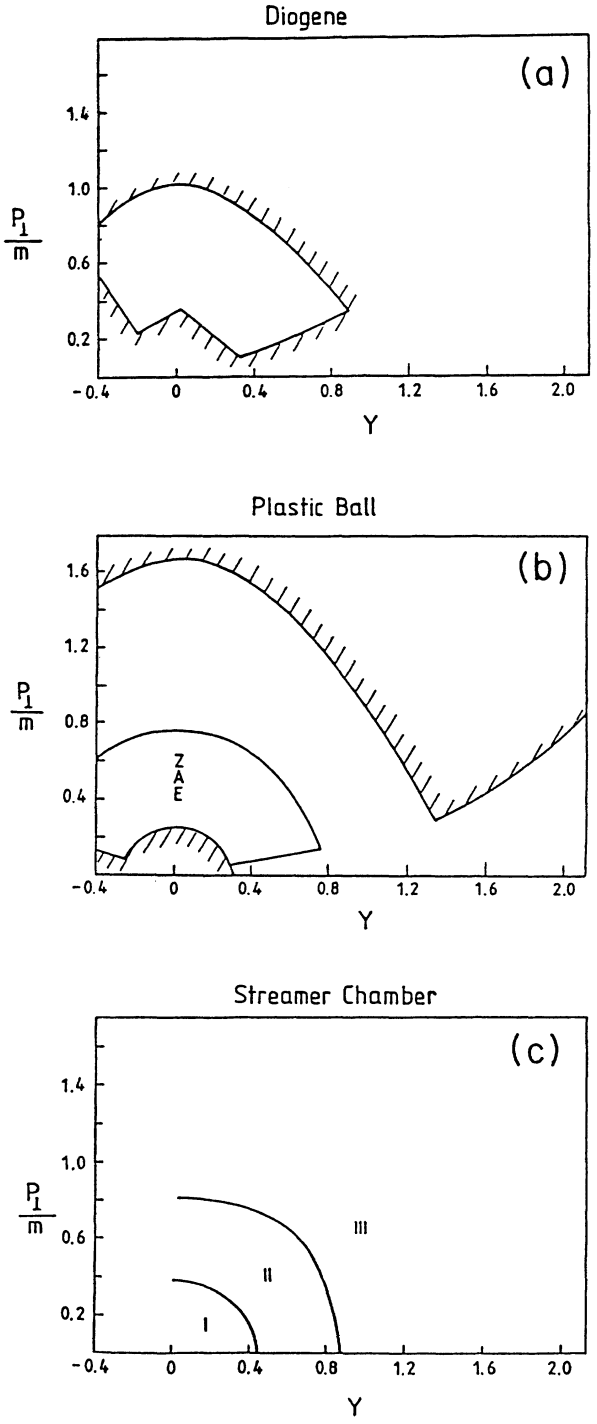

FIG. 7. Acceptance of the Diogene detector [13] (a), of the Plastic Ball [22] (b) and of this experiment (c). The Plastic Ball has full particle identification only in the region marked ZAE; in the other parts only the charge (Z) and the velocity(β) are measured. For the flow analysis all detected particles are used; the most probable mass is assigned whenever the energy measurement is not available. In the Streamer Chamber detector no separation of deuterons from protons is possible in the region labeled I; in region II all deuterons and ~70% of the protons are identified; at the highest laboratory momenta (region III) all protons and ~90% of the deuterons are identified.

In a recent paper on flow in Au+Au collisions [12] between 75 and 650 MeV/nucleon, the transverse flow velocity was found to increase strongly with beam energy below around 300 MeV/nucleon, with saturation above this energy. Direct comparison of our data with Diogene results [13] at 400 MeV/nucleon incident energy leads to good agreement (260±10 MeV/c compared to 270±10 MeV/c); only estimated systematic errors due to the uncertainty in impact parameter and acceptance effects are given. The shapes of the $\langle p_x \rangle(y)$ dependence at large rapidities are different, which may be due to the exclusion of fast forward low transverse momentum particles in the Diogene analysis. Another difference is observed in the intercept of $\langle p_x \rangle(y)$ with the p_x=0 axis. Before and after acceptance correction the Diogene group finds 0.25 and 0.35, respectively, whereas our analysis gives a value of 0.17 . To our knowledge the Diogene analysis assumes a (symmetric) Gaussian distribution of the inclusive proton rapidity spectrum (with respect to the c.m. system). If, however, the experimental distribution is asymmetric in asymmetric projectile/target configurations, the extrapolation to full phase space will shift the intercept to larger values.

In order to illuminate the difficulties of a comparison of Streamer Chamber, Diogene, and Plastic Ball data Figs. 7(a)–7(c) show the acceptances of the three detectors. The particles not seen by the Diogene detector at low transverse momenta are corrected for by extrapolating a three-dimensional Gaussian distribution, which is fitted to the triple-differential cross section in the acceptance, to the blind regions of the detector. The Plastic Ball has full particle identification only in the region labeled ZAE; at large laboratory momenta the most probable mass is assigned to the particles. The Streamer Chamber suffers from lacking particle identification mainly at low laboratory momenta [region labeled I in Fig. 7(c)], which affects only marginally the flow analysis in the forward hemisphere of the c.m.s. In region II all deuterons and ~ 70% of the protons are identified. At the highest momenta (region III) all protons and ~90% of deuterons are identified.

The transverse momentum analysis used here and described in Ref. [5] allows the determination of the momentum tensor, which characterizes the distribution of the momentum flow in terms of the average flow angle and aspect ratio, the latter being a measure of the elongation of the tensor $r = 2f_3/(f_1 + f_2)$ with f_i the lengths of the three main tensor axis. The results of such a calculation for central Ar+Pb collisions at the three energies are presented in Fig. 8 and Table I. We find little variation of the flow angle with incident energy. Again the strongest flow effects occur at 800 MeV/nucleon with a modest decline at the highest energy. The Plastic Ball findings for heavy mass symmetric systems exhibit qualitatively the same behavior [14], i.e., the flow angle saturates around 800 MeV/nucleon and decreases for higher beam energies. The Diogene group has preliminary data on Ar+Pb at 400 MeV/nucleon [13]. Their analysis, along slightly different lines, is based on two-dimensional fits of transverse momenta in and out of the event plane. The resulting flow angles [13] are about twice as large and the aspect ratios correspondingly a factor of 2 lower than in the present experiment for 400 MeV/nucleon data. At least part of this difference can be attributed to the different acceptances of the Streamer Chamber and Diogene. Also shown in Fig. 8 are results for the symmetric Ar+KCl system. No published data are available for the lowest energy. Between 800 and 1800 MeV/nucleon, the flow angle stays essentially constant. The magnitudes of the flow angle and the aspect ratio depend strongly on the c.m. velocity which in turn is not uniquely determined by the experiment. In addition to the aforementioned intercept of $\langle p_x \rangle(y)$ with $\langle p_x \rangle$=0, one may use the c.m. velocity defined by the vanishing sum of all longitudinal momenta. Our result for the c.m. velocity (computed from all particles with $p_\perp$⟨250 MeV/c to exclude spectators) is also given in Table I. At the two lower energies the differences are large. Our result on flow angles and aspect ratios is obtained using $y_{\text{intercept}}$ at $\langle p_x \rangle$=0 which we believe to be the most adequate. Using the the c.m. velocity as defined above would result in higher flow angles and lower aspect ratios (21.4, 32.5, 15.8, and 2.04, 1.58, 2.14 at 400, 800, 1800 GeV/nucleon, respectively).

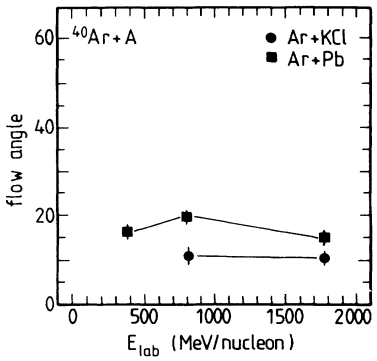

FIG. 8. Flow angle in degrees as a function of beam energy for central Ar+Pb and Ar+KCl [5, 6] collisions.

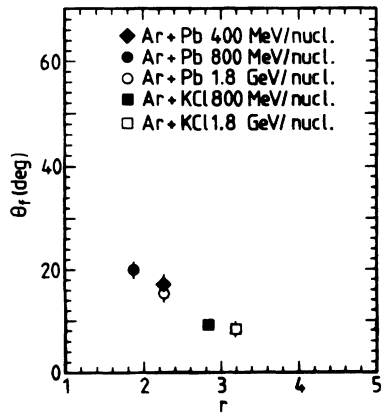

FIG. 9. Flow angle in degrees as a function of the aspect ratio $r = 2f_3/(f_1 + f_2)$ for central Ar+Pb and Ar+KCl [5, 6] collisions at 400, 800, and 1800 MeV/nucleon.

It is interesting to note that the variation of these flow parameters with the center-of-mass velocity seem to be restricted to a universal line in the plane span by the flow angle and the aspect ratio (r) as given in Fig. 9. A clear correlation between flow angle and elongation of the tensor emerges: independent of target size and beam energy the aspect ratio gets large for small flow angles and approaches 1 for large angles. Both the Diogene [15] and Plastic Ball [16] groups have reported flow effects perpendicular to the reaction plane. Our statistics do not allow such a detailed analysis, but the measured aspect ratios given in Table 1 and Ref. [5] are consistent with the findings of Refs. [15, 16].

The systematic errors of our experimental results are small enough to allow explicit and direct comparison with model calculations. In the past the results on $\langle p_x \rangle(y)$ from deuterons only in the Ar+Pb reaction at 800 MeV/nucleon [5], were compared to the transport model calculations with a hard equation of state [17, 18] and momentum dependent interactions [19], with the calculations only slightly underpredicting the data. With inclusion of protons into the experimental analysis the average in-plane transverse momenta drop by 20% at the highest rapidities bringing about closer agreement with the models. It appears that transport models which use a hard equation of state but lack the momentum dependent potential satisfactorily explain the data currently available. In general, the comparison of data with model calculations should be done at different incident energies simultaneously for the in-plane transverse momenta $\langle p_x \rangle(y)$ and rapidity distributions dn/dy [20] (or dP_x/dy [9]). This is, because the collective effects may be enhanced not only by the mean field but also by a higher degree of stopping [21] which in turn affects the rapidity distributions, particularily in asymmetric systems. So far studies of collective effects in experimental data and their comparison with model calculations were mostly done for symmetric target/projectile systems. We are confident that the present work, which gives experimental data on flow and rapidity distributions for protons and deuterons at three different energies, will supplement the information from the symmetric systems and constrain further the assumptions of the different theoretical approaches.

ACKNOWLEDGMENTS

We wish to thank J.P. Branningan, the BEVALAC staff, and the scanning and measuring staffs in Riverside and Heidelberg for their contribution to this work. P.D. acknowledges support by the National Science Foundation under Grant No. Phy-8905933 and No. Phy-90017077. This work was supported in part by the U.S. Department of Energy under Contract No. DE-AC03-76SF00098.

[1] H.-A.Gustafsson *et al.*, Phys. Rev. Lett. **52**, 1590 (1984); R.E. Renfordt *et al.*, *ibid.* **53**, 763 (1984); see also Ref. [4]. For reviews, see H.H. Gutbrod, A.M. Poskanzer, and H.G. Ritter, Rep. Prog. Phys. **52**, 1267 (1989); K.H. Kampert, J. Phys. G **15**, 691 (1989).

[2] G.F. Chapline , M.H. Johnson, E. Teller, and M.S. Weiss, Phys. Rev. D **8**, 4302 (1973); W. Scheid, H. Müller and W. Greiner, Phys. Rev. Lett. **32**, 741 (1974).

[3] See *Proceedings of the NATO Advanced Study Institute on the Nuclear Equation of State*, Peñiscola, Spain, edited by W. Greiner and H. Stöcker, NATO ASI Series B: Physics 216A (Plenum, New York, 1989).

[4] D. Beavis, S.Y. Chu, S.Y. Fung, W. Gorn, A. Huie, D. Keane, J.J. Lu, R.T. Poe, B.C. Chen, and D. VanDalen, Phys. Rev. C **27**, 2443 (1983).

[5] P. Danielewicz *et al.*, Phys. Rev. C **38**, 120 (1988).

[6] P. Danielewicz and G. Odyniec, Phys. Lett. **129B**, 146 (1985).

[7] R. Brockmann *et al.*, Phys. Rev. Lett. **53**, 2012 (1984).

[8] K.R. Doss *et al.*, Phys. Rev. Lett. **57**, 302 (1986).

[9] D. Beavis, S.Y. Chu, S.Y. Fung, W. Gorn, D. Keane, Y.M. Liu, D. VanDalen, and M. Vient, Phys. Rev. C **33**, 1113 (1986).

[10] H.A. Gustafsson, H.H. Gutbrod, J.W. Harris, B.V. Jacak, K.-H. Kampert, B. Kolb, A.M. Poskanzer, H.G. Ritter, and H.R. Schmidt, Mod. Phys. Lett. A **3**, 1323 (1988).

[11] C.A. Ogilvie *et al.*, Phys. Rev. C **40**, 2592 (1989).

[12] P.M. Zhang *et al.*, Phys. Rev. C **42**, R491 (1990).

[13] J. Gosset *et al.*, in *Proceedings of the NATO Advanced Study Institute on the Nuclear Equation of State* [3], p. 87; M. Demoulins, Ph.D. thesis, University of Paris, 1989; Report No. CEA-N-2628, 1990 (unpublished).

[14] H.G. Ritter *et al.*, in *Proceedings of the NATO Advanced Study Institute on the Nuclear Equation of State* [3], p. 31.

[15] M. Demoulins *et al.*, Phys. Lett. B **241**, 476 (1990).

[16] H.H. Gutbrod, K.-H. Kampert, B. Kolb, A.M. Poskanzer, H.G. Ritter, R. Schicker, and H.R. Schmidt, Phys. Rev. C **42**, 460 (1990).

[17] J.J. Molitoris and H. Stöcker, Phys. Lett. **162B**, 47 (1985).

[18] C. Hartnack, thesis, Universität of Frankfurt/Main, 1990; in *Proceedings of the NATO Advanced Study Institute on the Nuclear Equation of State* [3], p. 239.

[19] C. Gale, G.M. Welke, H. Prokash, S.Y. Lee, and S. Das Gupta, Phys. Rev. C **41**, 1545 (1990).

[20] D. Keane, S.Y. Chu, S.Y. Fung, Y.M. Liu, L.J. Qiao, G. VanDalen, M. Vient, S. Wang, J.J. Molitoris, and H. Stöcker, Phys. Rev. C **37**, 1447 (1988).

[21] G.F. Bertsch, G.E. Brown, V. Koch, and B.-A. Li, Nucl. Phys. **A490**, 745 (1988).

[22] A. Baden *et al.*, Nucl. Instrum. Methods **203**, 189 (1982).